

See discussions, stats, and author profiles for this publication at: <https://www.researchgate.net/publication/250920882>

Synthesis, Magnetism, and Electrochemistry of the Ni-14⁻ and Ni-5-Containing Heteropolytungstates [Ni-14(OH)(6)(H₂O)(10)(HPO₄)₄(P₂W₁₅O₅₆)₄]₍₃₄₋₎ and [Ni-5(OH)(4)(H₂O)₄]_(beta-G...)

ARTICLE *in* INORGANIC CHEMISTRY · JULY 2013

Impact Factor: 4.76 · DOI: 10.1021/ic400943j · Source: PubMed

CITATIONS

22

READS

544

8 AUTHORS, INCLUDING:



Masooma Ibrahim

Karlsruhe Institute of Technology

24 PUBLICATIONS 363 CITATIONS

[SEE PROFILE](#)



Bassem S Bassil

University of Balamand

108 PUBLICATIONS 2,220 CITATIONS

[SEE PROFILE](#)



Yanhua Lan

CNRS, Université Joseph Fourier et Grenoble INP

159 PUBLICATIONS 3,380 CITATIONS

[SEE PROFILE](#)

Annie K. Powell

Karlsruhe Institute of Technology

488 PUBLICATIONS 12,273 CITATIONS

[SEE PROFILE](#)

Synthesis, Magnetism, and Electrochemistry of the Ni_{14}^- and Ni_5^- -Containing Heteropolytungstates $[\text{Ni}_{14}(\text{OH})_6(\text{H}_2\text{O})_{10}(\text{HPO}_4)_4(\text{P}_2\text{W}_{15}\text{O}_{56})_4]^{34-}$ and $[\text{Ni}_5(\text{OH})_4(\text{H}_2\text{O})_4(\beta\text{-GeW}_9\text{O}_{34})(\beta\text{-GeW}_8\text{O}_{30}(\text{OH}))]^{13-}$

Masooma Ibrahim,^{†,||} Yixian Xiang,[†] Bassem S. Bassil,[†] Yanhua Lan,[§] Annie K. Powell,^{*,||,§} Pedro de Oliveira,[‡] Bineta Keita,[†] and Ulrich Kortz^{*,†}

[†]Jacobs University, School of Engineering and Science, P.O. Box 750 561, 28725 Bremen, Germany

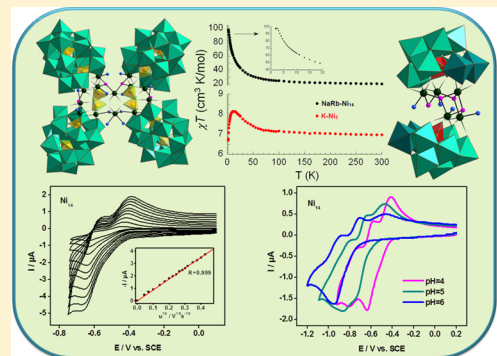
^{||}Institute of Nanotechnology, Karlsruhe Institute of Technology (KIT), Hermann-von-Helmholtz Platz 1, 76344 Eggenstein-Leopoldshafen, Germany

[§]Institute of Inorganic Chemistry, Karlsruhe Institute of Technology (KIT), Engesserstrasse 15, 76131 Karlsruhe, Germany

[‡]Laboratoire de Chimie Physique, UMR 8000, CNRS, Equipe d'Electrochimie et de Photoélectrochimie, Université Paris-Sud, Bâtiment 350, 91405 Orsay Cedex, France

Supporting Information

ABSTRACT: The two Ni^{2+} -containing heteropolytungstates $[\text{Ni}_{14}(\text{OH})_6(\text{H}_2\text{O})_{10}(\text{HPO}_4)_4(\text{P}_2\text{W}_{15}\text{O}_{56})_4]^{34-}$ (Ni_{14}) and $[\text{Ni}_5(\text{OH})_4(\text{H}_2\text{O})_4(\beta\text{-GeW}_9\text{O}_{34})(\beta\text{-GeW}_8\text{O}_{30}(\text{OH}))]^{13-}$ (Ni_5) have been successfully synthesized in aqueous, basic media under conventional reaction conditions, and they were characterized by single-crystal X-ray diffraction, IR spectroscopy, thermogravimetric and elemental analyses, electrochemistry, and magnetic studies. The cyclic voltammetry (CV) patterns of Ni_{14} and Ni_5 showed chemically reversible multielectronic waves for slow scan time scales. For Ni_{14} , an important acidity inversion effect between its reduced forms was observed. Magnetic studies revealed dominant ferromagnetic interactions among the nickel(II) ions in both polyanions.



INTRODUCTION

Polyoxometalates (POMs) are discrete inorganic anions with potential applications in a variety of fields, such as analytical chemistry, molecular magnetism, nanotechnology, medicine, electrochemistry, photochemistry, and catalysis.¹ POMs usually comprise octahedrally coordinated tungsten, molybdenum, or vanadium ions in high oxidation states, with the polyhedral shared via edges or corners.² Polyanions containing an additional, central element are known as heteropolyanions, such as the highly symmetrical Keggin ion $[\text{XW}_{12}\text{O}_{40}]^{9-}$ ($\text{X} = \text{Si}^{\text{IV}}, \text{Ge}^{\text{IV}}, \text{P}^{\text{V}}, \text{As}^{\text{V}}$, etc.). The Keggin ion is composed of a central, tetrahedral XO_4 hetero group surrounded by four edge-shared W_3O_{13} "triads". Another well-known planar structure is the Wells–Dawson ion $[\text{X}_2\text{W}_{18}\text{O}_{62}]^{6-}$ ($\text{X} = \text{P}^{\text{V}}, \text{As}^{\text{V}}$), which can be viewed as being constructed of two fused $[\text{A}-\alpha\text{-XW}_9\text{O}_{34}]^{n-}$ units. The Keggin and Wells–Dawson ions can be transformed, via base hydrolysis, to lacunary (vacant) derivatives by loss of one or more WO_6 octahedra.² The resultant structural defects or voids tremendously enhance the reactivity of POMs as multidentate oxo ligands toward various electrophiles, making them good candidates for the encapsulation of polynuclear d- and f-block metal–oxo fragments, leading to products with interesting magnetic and electrochemical properties.³ This

virtue of POMs can be related to organic polydentate ligands, which are also known to coordinate to transition metal ions.⁴ In this context, transition metal-containing polyanions represent a large subclass of POM chemistry, and the paramagnetic derivatives are particularly interesting.⁵

To date, many Ni^{2+} -containing POMs have been reported, most of them comprising less than 5 Ni^{2+} ions, but some larger nickel–oxo/hydroxo cores could also be constructed.^{6–16,19} To the best of our knowledge, the largest number of nickel ions incorporated in a Keggin-type POM is 12. Wang's group reported the dodecanickel(II)-containing 35-tungsto-3-phosphate(V) $[\text{Ni}_{12}(\text{OH})_9\text{WO}_4(\text{W}_7\text{O}_{26}(\text{OH}))(\text{PW}_9\text{O}_{34})_3]^{25-}$ (Ni_{12}), which was synthesized under reflux conditions.⁶ In this polyanion, three $\{\text{Ni}_4\text{-PW}_9\text{O}_{34}\}$ units are connected to each other via a WO_4 tetrahedron and a $[\text{W}_7\text{O}_{26}(\text{OH})]^{11-}$ fragment. The nonplanar nucleic trimeric polyanion $[\text{Ni}_9(\text{OH})_3(\text{H}_2\text{O})_6(\text{HPO}_4)_2(\text{PW}_9\text{O}_{34})_3]^{16-}$ (Ni_{9a}), reported by Coronado's group, consists of three $\{\text{Ni}_3\text{-PW}_9\text{O}_{34}\}$ units connected to each other by three hydroxo bridges and two central $(\text{HPO}_4)^{2-}$ groups.⁸ On the other hand, Mialane's group

Received: January 8, 2013

Published: July 19, 2013



Table 1. Crystal Data for NaRb-Ni₁₄ and K-Ni₅

	NaRb-Ni ₁₄	K-Ni ₅
empirical formula	Na _{32.5} Rb _{1.5} [{Ni ₁₄ (OH) ₆ (H ₂ O) ₁₀ (HPO ₄) ₄ (P ₂ W ₁₅ O ₅₆) ₄ }·109H ₂ O	K _{1.3} [Ni ₅ (OH) ₄ (H ₂ O) ₄ (GeW ₉ O ₃₄) ₄ (β-GeW ₈ O ₃₀ (OH))] ₃ ·32H ₂ O
formula wt, g/mol	19189.9	11660.2
cryst syst	triclinic	triclinic
space group	P <bar{1}< td=""><td>P<bar{1}< td=""></bar{1}<></td></bar{1}<>	P <bar{1}< td=""></bar{1}<>
<i>a</i> , Å	15.6062(5)	18.4924(4)
<i>b</i> , Å	24.9652(9)	21.8208(4)
<i>c</i> , Å	49.490(2)	25.2971(6)
α , deg	90.601(3)	81.7470(10)
β , deg	92.688(2)	73.8930(10)
γ , deg	90.439(2)	85.1010(10)
vol, Å ³	19258.9(12)	9694.4(4)
Z	2	2
D_{calcd} , g/cm ³	3.309	3.995
abs coeff	18.888	22.319
cryst size	0.40 × 0.13 × 0.12	0.20 × 0.16 × 0.09
theta range, deg	3.40–20.82	3.40–26.37
reflns collected	271892	230290
indep reflns	39724	39077
$R(\text{int})$	0.1449	0.1227
obsd ($I > 2\sigma(I)$)	23300	27241
goodness-of-fit on F ₂	1.008	1.004
$R_1[I > 2\sigma(I)]^a$	0.1067	0.0529
wR ₂ (all data) ^b	0.2772	0.1566

$$^a R = \sum |F_o| - |F_c| / \sum |F_o|. \quad ^b R_w = [\sum w(F_o^2 - F_c^2)^2 / \sum w(F_o^2)^2]^{1/2}.$$

and some of us reported the nonanuclear, dimeric, asymmetric polyanion $[\text{Ni}_9(\text{OH})_6(\text{H}_2\text{O})_6(\text{CO}_3)_3(\text{SiW}_9\text{O}_{34})_2]^{14-}$ (Ni_{9b}), which is composed of two $[\text{Ni}_4(\text{OH})_3(\text{SiW}_9\text{O}_{34})]^{5-}$ subunits connected by three carbonato ligands and an additional Ni²⁺ center.⁹ This group also reported the octa-Ni²⁺-substituted derivatives $[\text{Na}\{\text{Ni}_4(\text{CH}_3\text{COO})_3(\text{OH})_3(\text{SiW}_9\text{O}_{34})\}_2]^{15-}$ (Ni₈) and $[\text{Na}\{\text{Ni}_4(\text{CH}_3\text{COO})_3(\text{OH})_2(\text{N}_3)(\text{SiW}_9\text{O}_{34})\}_2]^{15-}$ (Ni₈N₃).⁹ These dimeric, octanuclear polyanions contain two $\{\text{Ni}_4(\text{SiW}_9\text{O}_{34})\}$ subunits linked via a $\{\text{Na}(\text{CH}_3\text{COO})_6\}$ group in Ni₈ and a $\{(\text{CH}_3\text{COO})_6(\text{N}_3)_2\}$ group in Ni₈N₃, with six μ -hydroxo ligands in Ni₈ being substituted by two azido ligands in Ni₈N₃. Wang's group also synthesized a hepta- and a hexa-Ni^{II}-substituted derivative, $[\text{Ni}_7(\text{OH})_4(\text{H}_2\text{O})(\text{CO}_3)_2(\text{HCO}_3)-(\text{SiW}_9\text{O}_{34})(\text{SiW}_{10}\text{O}_{37})]^{10-}$ (Ni_{7a}) and $[\{\text{Ni}_6(\text{H}_2\text{O})_4(\mu_2\text{-H}_2\text{O})_4(\mu_3\text{-OH})_2\}(\text{SiW}_9\text{O}_{34})_2]^{10-}$ (Ni₆), respectively. The former consists of $[\text{SiW}_9\text{O}_{34}]^{10-}$ and $[\text{SiW}_{10}\text{O}_{37}]^{10-}$ units linked by a $\{\text{Ni}_7\}$ core and three carbonate ions, whereas in the latter the $\{\text{Ni}_6\}$ core is stabilized by two $[\text{SiW}_9\text{O}_{34}]^{10-}$ units.¹⁰ The same group also reported the hepta-Ni²⁺-substituted, dimeric species $[\text{Ni}_7(\text{OH})_6(\text{H}_2\text{O})_4(\text{SiW}_8\text{O}_{31})_2]^{12-}$ (Ni_{7b}) and the penta-Ni²⁺-substituted, dimeric, asymmetric $[\text{H}_2\{\text{Ni}_5(\text{OH})_3(\text{H}_2\text{O})_5(\text{SiW}_9\text{O}_{34})(\text{SiW}_8\text{O}_{31})\}_2]^{24-}$.¹¹ Hybrid organic-inorganic POMs based on a single trivacant Keggin fragment capped by a hexa-Ni²⁺ or hepta-Ni²⁺ unit have also been synthesized under hydrothermal conditions.¹² Several other classical nickel-containing sandwich and monomeric structures based on lacunar Keggin ions have also been reported.¹³ Very recently, Yang's group prepared a series of solid state POM assemblies comprising between 20 and 40 Ni centers, by using hydrothermal conditions and in the presence of organic amines (ethylenediamine, 1,2-diaminopropane).⁶ These compounds were synthesized by interaction of nickel(II) salts with different lacunar Keggin-type precursors in the presence of the respective amine, leading to symmetrical (two identical POM

caps) as well as unsymmetrical (two different POM caps) sandwich derivatives.

Several Ni-containing Wells-Dawson-based polyanions are also known, but the number is smaller than for the Keggin system. Cronin's group reported $[(\text{Ni}_2\text{P}_2\text{W}_{16}\text{O}_{50})_3]^{30-}$ (Ni₆), which is a trimeric polyanion containing six Ni²⁺ centers in a structure comprising three dinickel(II)-substituted $[\text{Ni}_2\text{P}_2\text{W}_{16}\text{O}_{60}]^{10-}$ fragments linked via six $\{\text{Ni}-\text{O}-\text{W}\}$ bridges.¹⁴ Wang's group reported a crown-type macrocyclic polyanion with 6 Ni²⁺ ions inside the triangular $\{(\text{WO}-(\text{H}_2\text{O})_3(\text{P}_2\text{W}_{12}\text{O}_{48})_3\}^{18-}$ host.¹⁵ Reaction of the trilacunary Wells-Dawson ion $[\text{P}_2\text{W}_{15}\text{O}_{56}]^{12-}$ with nickel(II) ions has resulted in Weakley-type sandwich structures, such as $[\text{Na}\{\text{Ni}_3(\text{H}_2\text{O})_2(\text{P}_2\text{W}_{15}\text{O}_{56})_2\}]^{17-}$, $[\text{Co}\{\text{Ni}_3(\text{H}_2\text{O})_2(\text{P}_2\text{W}_{15}\text{O}_{56})_2\}]^{16-}$, and $[\text{Ni}_4(\text{H}_2\text{O})_2(\text{P}_2\text{W}_{15}\text{O}_{56})_2]^{16-}$.¹⁶ The macrocyclic 48-tungsto-8-phosphate $[\text{H}_7\text{P}_8\text{W}_{48}\text{O}_{184}]^{33-}$ ¹⁷ has attracted much attention in recent years, in particular after the report on $[\text{Cu}_{20}\text{Cl}(\text{OH})_{24}(\text{H}_2\text{O})_{12}(\text{P}_8\text{W}_{48}\text{O}_{184})]^{25-}$,¹⁸ and has resulted in the nickel(II)-containing $[\text{Ni}_4(\text{H}_2\text{O})_{16-}(\text{P}_8\text{W}_{48}\text{O}_{184})(\text{WO}_2(\text{H}_2\text{O})_2)]^{28-}$.¹⁹

Here we report on the synthesis of novel Ni₅- and Ni₁₄-containing heteropolyanions, as well as their magnetic and electrochemical properties.

EXPERIMENTAL SECTION

General Methods and Materials. All reagents were used as purchased without further purification. The trilacunary tungstophosphate precursor salt Na₁₂[P₂W₁₅O₅₆]·24H₂O was prepared by Finke's procedure,²⁰ and the dilacunary tungstogermanate precursor salt K₈[γ -GeW₁₀O₃₆]·6H₂O by Kortz's procedure.²¹ The purity of both compounds was confirmed by infrared spectroscopy.

Synthesis of Na_{32.5}Rb_{1.5}[Ni₁₄(OH)₆(H₂O)₁₀(HPO₄)₄-(P₂W₁₅O₅₆)₄]·109H₂O (NaRb-Ni₁₄). NiCl₂·6H₂O (0.15 g, 0.63 mmol) was dissolved in 20 mL of H₂O. Then solid Na₁₂[P₂W₁₅O₅₆]·18H₂O (0.86 g, 0.20 mmol) was added, and the mixture was stirred until a clear, green solution was obtained. The pH

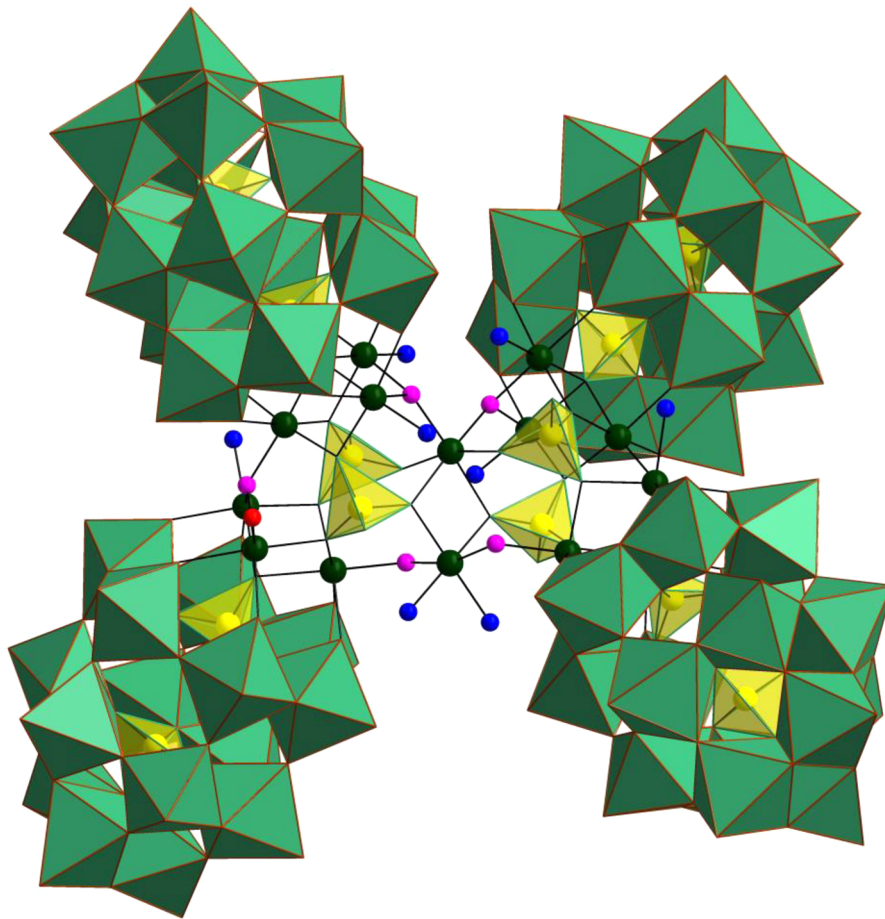


Figure 1. Combined polyhedral/ball-and-stick representation of Ni_{14} . Color code: WO_6 octahedra (green), PO_4 tetrahedra (yellow), Ni (dark green), OH (pink), H_2O (blue).

of the resulting mixture was adjusted to 8.0 with 4 M NaOH, and the mixture was stirred for 10 min at room temperature. Then solid Na_3PO_4 (0.50 g, 3.0 mmol) was added to this solution in small portions, while the pH was maintained at 8 with HCl_{aq} . The mixture was stirred at room temperature for 1 h, and then the precipitate was allowed to settle down, followed by filtration and addition of 0.20 mL of 1 M RbCl solution. Slow evaporation at room temperature led to the appearance of green, crystalline NaRb-Ni_{14} after about 10 days, which was filtered off and air-dried. Yield: 0.40 g (42%). IR (2% KBr pellet, ν/cm^{-1}): 1085(s), 1051(m), 1011(w), 938(m), 912(w), 880(w), 813(s), 728(s), 599(w), 562(w), 520(s), 458(w). Elemental analysis (%) calc (found): Rb 0.67 (0.62), Na 3.90 (4.13), Ni 4.28 (4.26), W 57.5 (55.0), P 1.94 (2.04).

Synthesis of $\text{K}_{13}[\text{Ni}_5(\text{OH})_4(\text{H}_2\text{O})_4(\beta\text{-GeW}_9\text{O}_{34})(\beta\text{-Ge-W}_8\text{O}_{30}(\text{OH}))]\cdot32\text{H}_2\text{O}$ (K-Ni_5). 0.16 g (0.63 mmol) of $\text{Ni}(\text{OAc})_2\cdot4\text{H}_2\text{O}$ were dissolved in 20 mL of distilled water, and then 0.58 g (0.20 mmol) of $\text{K}_8[\gamma\text{-GeW}_{10}\text{O}_{36}]\cdot6\text{H}_2\text{O}$ were added. The pH of the resulting clear, green solution was adjusted to 8 by using 2 M K_2CO_3 , and then it was left stirring at room temperature for 1 h. The resultant turbid solution was filtered, and slow evaporation of the filtrate resulted in green crystals of K-Ni_5 after about three weeks. Yield 0.05 g (9%). IR (2% KBr pellet, ν/cm^{-1}): 936 (s), 871 (m), 791 (s), 694 (m), 550 (w), 458 (s). Elemental analysis (%) calc (found): K 8.72 (8.30), Ni 5.03 (5.33), W 53.6 (52.8), Ge 2.49 (2.59).

IR, TGA, and Elemental Analysis. Infrared (IR) spectra were recorded on a Nicolet Avatar 370 FT-IR spectrophotometer using KBr pellets. The following abbreviations were used to assign the peak intensities: w = weak, m = medium, and s = strong. Elemental analyses for NaRb-Ni_{14} and K-Ni_5 were performed by CNRS, Service Central d'Analyse, Solaize, France. Thermogravimetric analyses (TGA) were carried out on a TA Instruments SDT Q600 thermobalance with a 100

mL/min flow of nitrogen; the temperature was ramped from 20 to 1000 °C at a rate of 5 °C/min.

X-ray Crystallography. The crystals were mounted on a Hampton cryoloop in light oil for data collection at 173 K. Indexing and data collection were performed on a Bruker D8 SMART APEX II CCD diffractometer with kappa geometry and Mo $\text{K}\alpha$ radiation (graphite monochromator, $\lambda = 0.71073 \text{ \AA}$). Data integration was performed using SAINT.²² Routine Lorentz and polarization corrections were applied. Multiscan absorption corrections were performed using SADABS.²³ Direct methods (SHELXS97) successfully located the tungsten atoms, and successive Fourier syntheses (SHELXL97) revealed the remaining atoms.²⁴ Refinements were full-matrix least-squares against $|F^2|$ using all data. In the final refinement, all non-disordered heavy atoms (W, Ni, Ge, P, Rb, K) were refined anisotropically; oxygen atoms and disordered counter cations were refined isotropically. No hydrogen atoms were included in the models. For overall consistency we show in the CIF files the same formula units as in the text with the exact numbers of counter cations and crystal waters (based on elemental analysis and TGA), as this reflects the true bulk composition of NaRb-Ni_{14} and K-Ni_5 . Crystallographic data are summarized in Table 1.

Magnetic Susceptibility Measurements. The magnetic susceptibility measurements were obtained on a Quantum Design SQUID magnetometer MPMS-XL. This magnetometer works between 1.8 and 400 K for dc applied fields ranging from -7 to 7 T. Measurements were performed on polycrystalline samples of 33.0 mg of NaRb-Ni_{14} and 30.8 mg of K-Ni_5 , respectively. For both compounds ac susceptibility measurements were also performed, with an oscillating ac field of 3 Oe and ac frequencies at 1000 Hz, but the out-of-phase component was found to be absent. The magnetic data were corrected for the sample holder and diamagnetic contributions.

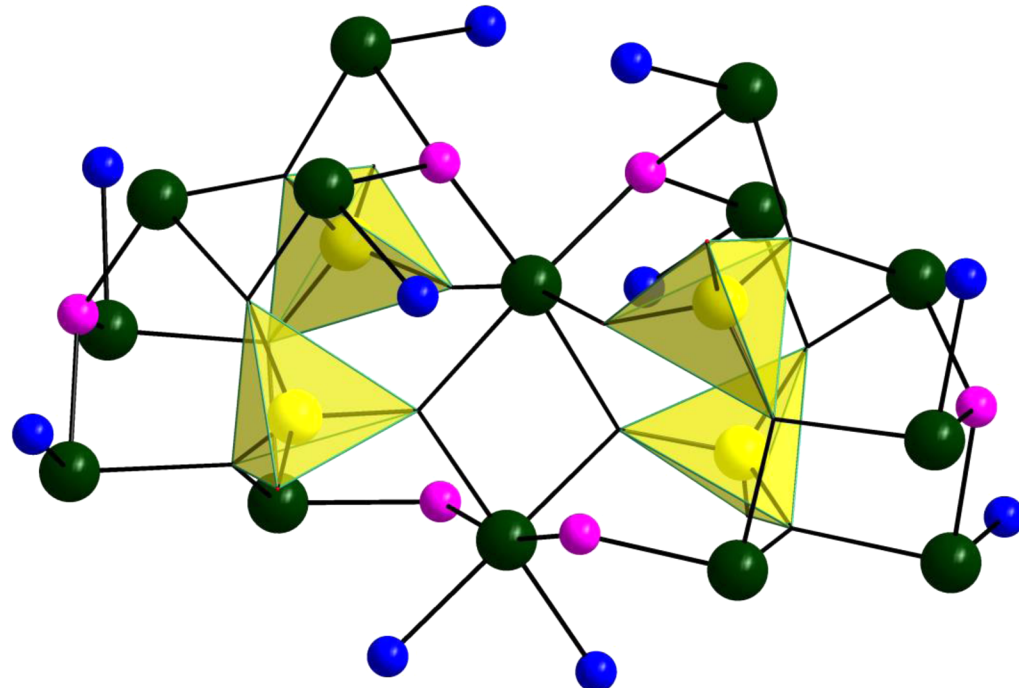


Figure 2. Ball-and-stick representation of the $[(\text{Ni}_{14}(\text{OH})_6(\text{H}_2\text{O})_{10}(\text{HPO}_4)_4]^{14+}$ core in Ni_{14} . The color code is the same as in Figure 1.

Electrochemical Experiments. The electrochemical setup was an EG & G 273 A driven by a PC with the M270 software. Potentials are quoted against a saturated calomel electrode (SCE). The counter electrode was a platinum gauze of large surface area. All experiments were performed at room temperature. The source, mounting, and polishing of the glassy carbon (Le Carbone-Lorraine) electrodes have been described.²⁵ The glassy carbon samples had a diameter of 3 mm. The solutions were deaerated thoroughly for at least 30 min with pure argon and kept under a positive pressure of this gas during the experiments. Spectra were recorded with a Lambda 19 Perkin-Elmer spectrophotometer. The solutions were placed in quartz cuvettes with an optical path of 0.2 cm. The composition and pH of the media used for both the electrochemical experiments and the stability studies by spectrophotometry were as follows: 1 M $\text{LiCH}_3\text{COO}/\text{CH}_3\text{COOH}$ (pH 4, 5, 6); 0.4 M $\text{NaH}_2\text{PO}_4/\text{NaOH}$ (pH 7).

RESULTS AND DISCUSSION

Synthesis and Structure. The Ni_{14} -Containing $[\text{Ni}_{14}(\text{OH})_6(\text{H}_2\text{O})_{10}(\text{HPO}_4)_4(\text{P}_2\text{W}_{15}\text{O}_{56})_4]^{34-}$ (Ni_{14}). The 14-nickel(II)-containing 60-tungsto-12-phosphate $[\text{Ni}_{14}(\text{OH})_6(\text{H}_2\text{O})_{10}(\text{HPO}_4)_4(\text{P}_2\text{W}_{15}\text{O}_{56})_4]^{34-}$ (Ni_{14}) was synthesized in a one-pot reaction of the trilacunary polyanion precursor $[\text{P}_2\text{W}_{15}\text{O}_{56}]^{12-}$ with Ni^{2+} ions in a phosphate buffer at pH 8. The novel Ni_{14} crystallized as the hydrated sodium–rubidium salt $\text{Na}_{31.5}\text{Rb}_{1.5}[\text{Ni}_{14}(\text{OH})_6(\text{H}_2\text{O})_{10}(\text{HPO}_4)_4(\text{P}_2\text{W}_{15}\text{O}_{56})_4]\cdot10\text{H}_2\text{O}$ (NaRb-Ni_{14}) in the triclinic space group $P\bar{1}$. Single crystal X-ray diffraction analysis on NaRb-Ni_{14} revealed that the polyanion is composed of two $\{\text{(Ni}_3\text{O}_2\text{OH})(\text{P}_2\text{W}_{15}\text{O}_{56})\}$ subunits (denoted $\{\text{Ni}_3\text{-OH}\}$), two $\{\text{(Ni}_3\text{O}_2)(\text{P}_2\text{W}_{15}\text{O}_{56})\}$ subunits (denoted $\{\text{Ni}_3\text{-O}\}$), and a central $\{\text{Ni}_2(\text{OH})_4(\text{H}_2\text{O})(\text{PO}_4)_4\}$ assembly (denoted $\{\text{Ni}_2\}$), see Figure 1. As expected, three nickel ions occupy the vacant site of each trilacunary Wells–Dawson ion. Each $\{\text{Ni}_3\text{-OH}\}$ subunit is connected to a $\{\text{Ni}_3\text{-O}\}$ subunit by two $\text{Ni}-\text{OH}-\text{Ni}$ bridges. The resulting two dimeric assemblies are connected to the central $\{\text{Ni}_2\}$ group. As a result, the two Ni^{2+} ions in $\{\text{Ni}_2\}$ are in different coordination environments, with one of them connecting two Wells–Dawson units via two $\mu_3\text{-OH}$ groups,

and the other bridging the remaining two Wells–Dawson units by two $\mu_2\text{-OH}$ groups, resulting in two terminal aqua ligands (Figure 2). The structure of Ni_{14} , besides being unprecedented, is also asymmetric, with idealized C_2 point group symmetry (the C_2 axis passing through the two nickel ions of the central $\{\text{Ni}_2\}$ group). The previously reported, structurally related, tetrameric polyanions have the transition metal substituted Keggin or Wells–Dawson subunits connected via either $\text{M}-\text{O}-\text{M}$ bridges^{26,27d} or phosphate linkers.²⁷

The presence of four phosphate groups is crucial for the formation of Ni_{14} . The structure-stabilizing effect of small anions such as phosphate is well-known in POM chemistry.^{7,8,27,28} The coordination environments of the four capping phosphate groups in Ni_{14} are not all equivalent, as two of them (P10 and P11) are coordinated to three $\mu_3\text{-oxo}$ bridges and a terminal hydroxo ligand, whereas the other two (P9 and P12) are coordinated to only two $\mu_3\text{-oxo}$ bridges, a $\mu_2\text{-oxo}$ bridge, and a terminal hydroxo ligand (all these bridges connect to nickel centers, see Figure 2). The 14 Ni^{2+} ions in Ni_{14} are coordinated by six oxygen atoms in idealized octahedral geometry with $\text{Ni}-\text{O}$ bond lengths in the range 1.98(4)–2.19(4) Å and $\text{O}-\text{Ni}-\text{O}$ bond angles in the range 78.7(14)–178.3(16)°. Bond valence sum (BVS) calculations²⁹ indicate the presence of six monoprotonated oxygens (two μ_2 and four μ_3 bridging OH) and 10 terminal diprotonated oxygens (aqua) in the 14-nickel core of polyanion Ni_{14} (Figures 1 and 2). The BVS value ranges for mono- and diprotonated oxygens are 0.70–1.15 and 0.32–0.40, respectively. Moreover, all the phosphate caps have a terminal hydroxo group each, with a BVS range of 1.09–1.28. In Table S1 in the Supporting Information the BVS values for all protonated oxygens in Ni_{14} are listed. Polyanion Ni_{14} can hence be described as comprising a cationic $[(\text{Ni}_{14}(\text{OH})_6(\text{H}_2\text{O})_{10}(\text{PO}_3\text{OH})_4]^{14+}$ core stabilized by four trilacunary $[\text{P}_2\text{W}_{15}\text{O}_{56}]^{12-}$ units. This leads to a total charge of 34– for Ni_{14} , which is balanced by 32.5 sodium and 1.5 rubidium counter cations in the solid state. In addition,

partial α/β disorder was observed crystallographically on the W_3O_{13} "cap" of the $\{P_2W_{15}\}$ units, with the β -conformation disorder ranging from 5% for the W31/W32/W33 triad to 20% for the W46/W47/W48 one. This disorder is limited to the triad cap and does not protrude to the rest of the polyanion structure, and could hence be easily modeled using partial occupancies of the affected atoms. The number of counter cations was determined by elemental analysis (see Experimental Section), whereas the number of water molecules was determined by thermogravimetric analysis (TGA). To the best of our knowledge, the title polyanion Ni_{14} contains the largest coherent nickel–oxo cluster known to date in polyoxotungstate chemistry. It should be realized that the previously reported solid state polytungstate assemblies with "20–40" Ni^{2+} ions (vide supra) do not contain coherent nickel–oxo cores, but contain rather two or more isolated, smaller clusters, and hence these species do not represent discrete polyanions.⁶ These materials were synthesized under hydrothermal conditions, and no solution studies were reported (most likely due to lack of solubility/stability).

The Ni_5 -Containing $[Ni_5(OH)_4(H_2O)_4(\beta-GeW_9O_{34})/\beta-GeW_8O_{30}(OH)]^{13-}$ (Ni_5). Interaction of Ni^{2+} ions with the dilacunary precursor $[\gamma-GeW_{10}O_{36}]^{8-}$ in a 3:1 ratio in aqueous pH 8 medium resulted in the penta- Ni^{2+} -containing, dimeric polyanion $[Ni_5(OH)_4(H_2O)_4(\beta-GeW_9O_{34})\{\beta-GeW_8O_{30}(OH)\}]^{13-}$ (Ni_5 , see Figure 3). This polyanion crystallized as a hydrated potassium salt $K_{13}[Ni_5(OH)_4(H_2O)_4(\beta-GeW_9O_{34})(\beta-GeW_8O_{30}(OH))] \cdot 32H_2O$ ($K-Ni_5$) in the triclinic space group $P\bar{1}$. Single crystal X-ray analysis of $K-Ni_5$ revealed two isolated, discrete Ni_5 polyanions, each comprising a hydroxo-bridged penta-nickel(II) moiety capped by a trilacunary $[\beta-GeW_9O_{34}]^{10-}$ and a tetralacunary $[\beta-GeW_8O_{31}]^{24-}$.

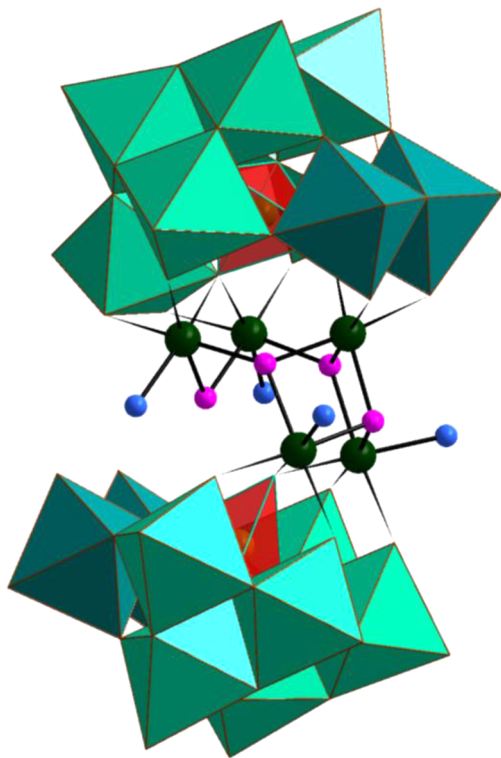


Figure 3. Combined polyhedral/ball-and-stick representation of Ni_5 . Color code: WO_6 octahedra (green), rotated WO_6 octahedra (teal), GeO_4 tetrahedra (red), Ni (dark green), OH (pink), H_2O (blue).

$W_8O_{30}(OH)]^{9-}$ Keggin unit, resulting in a structure with idealized C_s point group symmetry (Figure 3). Considering that Ni_5 was prepared by using the dilacunary, metastable γ -Keggin isomer $[\gamma-GeW_{10}O_{36}]^{8-}$, the $[\beta-GeW_9O_{34}]^{10-}$ and $[\beta-GeW_8O_{30}(OH)]^{9-}$ fragments must have been generated in situ by isomerization (rotation of edge-shared WO_6 octahedra) accompanied by loss of one or two WO_6 octahedra, respectively. Such transformations are not unprecedented in the chemistry of $[\gamma-XW_{10}O_{36}]^{8-}$ ($X = Ge, Si$).^{26b,30} The novel polyanion Ni_5 can also be described as a dimer, consisting of a tri- Ni^{2+} -substituted β -Keggin-unit $\{\beta-Ni_3GeW_9O_{34}\}$ linked by three μ_3 -OH groups to a di- Ni^{2+} -substituted γ -Keggin unit $\{\gamma-Ni_2GeW_8O_{31}\}$ (Figure 3). The interesting aspect here is that this linkage results in an edge-shared assembly of three NiO_6 octahedra.

The $[\beta-GeW_9O_{34}]^{10-}$ unit is composed of a central, tetrahedral GeO_4 hetero group which is surrounded by two equivalent $\{W_3O_{13}\}$ triads, a rotated $\{W_2O_{10}\}$ diad, and a $\{WO_6\}$ octahedron. The lacunary sites in this unit are occupied by three nickel(II) ions resulting in a $\{\beta-Ni_3GeW_9O_{34}\}$ unit. In the $[\beta-GeW_8O_{30}(OH)]^{9-}$ unit the single $\{WO_6\}$ octahedron mentioned above is missing. Two nickel ions occupy two formally rotated, edge-shared vacancies resulting in a $\{\gamma-Ni_2GeW_8O_{31}\}$ assembly (Figure 3). This motif was first seen in $[H_2\{Ni_5(H_2O)_5(OH)_3(\beta-SiW_9O_{34})(\beta-SiW_8O_{31})\}_2]^{24-}$, reported by Wang's group.¹¹ Our group has already reported other examples of sandwich-type polyanions containing a $\{\beta-XW_9O_{34}\}$ and a $\{\beta-XW_8O_{31}\}$ unit ($X = Si, Ge$), such as the tricobalt(II) containing 17-tungsto-2-silicate in $[Co_3(H_2O)(\beta-SiW_9O_{33}(OH))(\beta-SiW_8O_{29}(OH)_2)]^{11-}$, and the trimanganese(II) containing 17-tungsto-2-germanate $[Mn(H_2O)_2\{Mn_3(H_2O)(\beta-GeW_9O_{33}(OH))(\beta-GeW_8O_{30}(OH))\}]^{22-}$.³¹

Bond valence sum (BVS) calculations²⁹ on Ni_5 confirmed that the terminal oxygens of Ni are all diprotonated, and all μ_3 - and μ_2 -oxo ligands bridging the nickel ions are monoprotonated, resulting in a $[Ni_5(OH)_4(H_2O)_4]^{6+}$ magnetic core, stabilized by a $[\beta-GeW_9O_{34}]^{10-}$ and a $[\beta-GeW_8O_{30}(OH)]^{9-}$ unit (Figure 4). The protonation within the $[\beta-GeW_8O_{30}(OH)]^{9-}$ unit occurs at oxygens bridging two tungstens, namely, W1–O–W3 (BVS 1.11) for one of the two polyanions in the asymmetric unit, and W19–O–W21 (BVS 1.37) for the

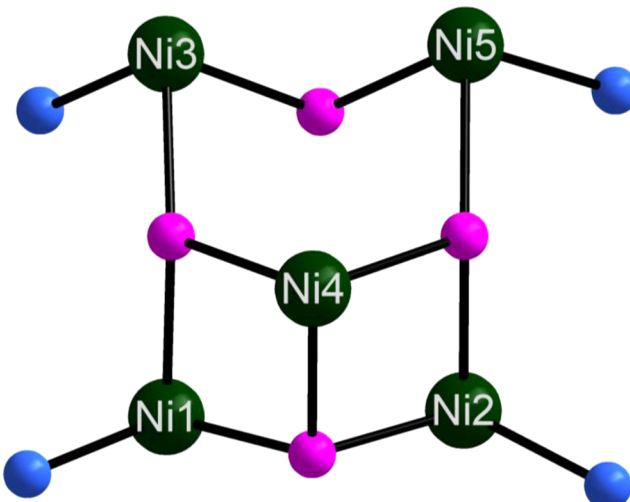


Figure 4. Ball-and-stick representation of the $[Ni_5(OH)_4(H_2O)_4]^{6+}$ core in Ni_5 . The color code is the same as in Figure 3.

other. Table S2 in the Supporting Information lists the BVS values for all protonated oxygens in Ni_5 . The total charge of Ni_5 is therefore 13 $-$, which is balanced by 13 potassium counter cations in the solid state. All the Ni^{2+} centers are hexacoordinated with a distorted octahedral geometry. The Ni–O bond lengths and O–Ni–O bond angles are in the ranges 2.010(13)–2.150(11) Å and 76.2(5)–177.7(5) $^\circ$, respectively.

Thermogravimetric analysis (TGA) was performed on K- Ni_5 in order to estimate the number of crystal waters per formula unit, and we identified ca. 32 water molecules (Figure S4 in the Supporting Information). It should be noted that the TGA data for NaRb- Ni_{14} as well as K- Ni_5 (Figures S3 and S4 in the Supporting Information) showed a lower amount of crystal water compared to the results of elemental analysis (97 vs 109 for NaRb- Ni_{14} and 29 vs 32 for K- Ni_5). This can be explained by the fact that the samples used for TGA measurements were dried slightly more than those used for elemental analysis.

Magnetic Measurements. Solid state dc susceptibility measurements on both compounds NaRb- Ni_{14} and K- Ni_5 were performed in the temperature range 1.8–300 K under a field of 1000 Oe. Plots of the product of the magnetic susceptibility and temperature versus temperature for NaRb- Ni_{14} and K- Ni_5 are shown in Figure 5. The χT product for both continuously

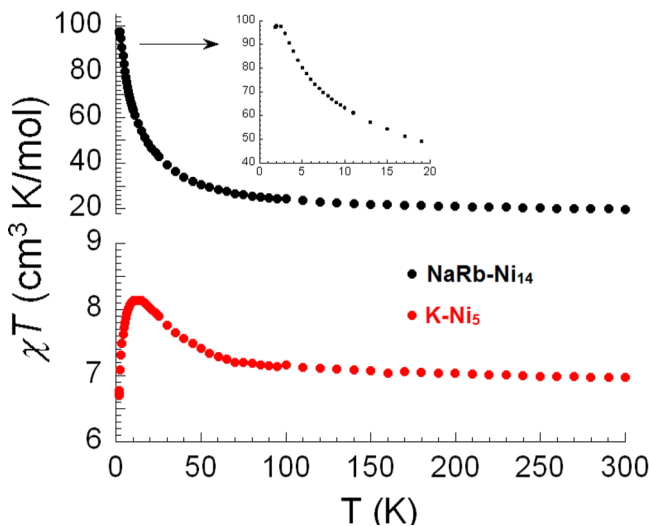


Figure 5. Temperature dependence of the χT products of NaRb- Ni_{14} and K- Ni_5 at 1000 Oe.

increases to reach a maximum and then rapidly drops on lowering the temperature. This type of behavior suggests the presence of dominant ferromagnetic interactions within both clusters. The final decrease of the χT product is due to the presence of magnetic anisotropy of the Ni^{2+} ions or possibly weak antiferromagnetic interactions. The χT product at 300 K is $19.61 \text{ cm}^3 \text{ K/mol}$ for NaRb- Ni_{14} and $6.97 \text{ cm}^3 \text{ K/mol}$ for K- Ni_5 , respectively. These values are consistent with those for 14 and 5 uncoupled Ni^{2+} ions with $g \approx 2.36$. Upon lowering the temperature, the χT product reaches a maximum value of $97.66 \text{ cm}^3 \text{ K/mol}$ for NaRb- Ni_{14} at 2.2 K and $8.14 \text{ cm}^3 \text{ K/mol}$ at 11 K for K- Ni_5 , respectively (see the inset in Figure 5). These maxima suggest a ground spin state of 13 for NaRb- Ni_{14} (assuming $g = 2.07$) and 3 for K- Ni_5 (assuming $g = 2.32$), both lower than the expected $S = 14$ ($105 \text{ cm}^3 \text{ K/mol}$) and $S = 5$ ($15 \text{ cm}^3 \text{ K/mol}$) values with $g = 2$, if all spins were coupled ferromagnetically. This suggests that antiferromagnetic inter-

actions are in competition with ferromagnetic ones within the cores. Examining the structures, it can be seen that in both compounds the Ni^{2+} ions are mostly bridged via μ_3 -oxo groups into triangular arrangements with the Ni–O–Ni angles ranging from $89.576(4)^\circ$ to $124.757(5)^\circ$ for Ni_{14} and $94.010(2)^\circ$ to $129.718(2)^\circ$ for Ni_5 , respectively. Based on experimental and theoretical studies on Ni^{2+} -containing polyoxoanions,^{7,8} it is well-known that Ni–Ni ferromagnetic exchange pathways are dominant when the Ni–O–Ni angles are in the range $90 \pm 14^\circ$. In both Ni_{14} and Ni_5 , some Ni–O–Ni angles are 120° or even larger, which should mediate antiferromagnetic interactions. Therefore, we can expect the coexistence of both ferro- and antiferromagnetic couplings in both polyanions. In spite of many attempts to model the magnetic susceptibility data, this did not prove possible. This may be because of the following: (a) there are at least three or even more coupling pathways present between adjacent Ni^{2+} ions; (b) intertriangle exchange between different Ni_3 triangles is not negligible; (c) the dominant ferromagnetic interactions are not significantly larger in magnitude than the antiferromagnetic ones; (d) the local single-ion anisotropy of the Ni^{2+} ions cannot be excluded from the exchange Hamiltonian.

UV–Visible Spectroscopy and Stability Studies. Both Ni_{14} and Ni_5 exhibit a broad band in the near-UV region of the spectrum. In the case of Ni_{14} , the band is at 260 nm in 1 M lithium acetate, pH 4 (ϵ_{\max} ca. $2 \times 10^5 \text{ M}^{-1} \text{ cm}^{-1}$), and blue shifts to 254 nm upon increasing the pH to 6. The band of Ni_5 clearly has a smaller extinction coefficient (ϵ_{\max} ca. $8 \times 10^4 \text{ M}^{-1} \text{ cm}^{-1}$ at 260 nm). Another broad band with a very weak absorbance is detected at 700 nm for both polyanions and is attributed to the Ni centers (Figure S5 in the Supporting Information).³²

Before studying the redox properties, it was necessary to determine the stability of Ni_{14} and Ni_5 in these electrolytes. In fact, it is known that polyanions may undergo chemical transformations or completely decompose depending on the pH of the solution in which they are dissolved. This was checked by recording and comparing their UV–vis spectra over a period matching the duration of an electrochemical experiment (which may last up to several hours). The stabilities of Ni_{14} and Ni_5 were assessed in several media. The polyanions were considered stable when the evolution of their spectra with time was negligible for at least 5 h, a period of time considered to be long enough to carry out a complete electrochemical experiment. Comparatively, Ni_5 is far less stable than Ni_{14} . The most favorable electrolytes are phosphate medium at pH 7 for Ni_5 and acetate media (pH ranging from 4 to 6) for Ni_{14} . A complementary cross-check of the stabilities of Ni_{14} and Ni_5 was obtained by cyclic voltammetry experiments (vide infra).

Electrochemistry. The electrochemistry of Ni_{14} and Ni_5 was carried out in various aqueous solutions. For this purpose, the stabilities of the two polyanions, in these media, were assessed by monitoring their respective UV–visible spectra. A complementary cross-check of this stability was obtained by cyclic voltammetry (CV). Only the tungsten centers are expected to give rise to an electrochemical response, with the Ni^{2+} ions being silent at our experimental conditions.³³

In a phosphate pH 7 medium, the CV of Ni_5 exhibits a sharp reduction wave at -1.254 V vs SCE, which is very close to the solvent discharge (Figure S6A in the Supporting Information). The characteristics of this chemically reversible W-wave undergo progressive transformation. The voltammograms recorded at different times show that the polyanion evolves:

the currents of all waves regularly increase, and an additional reduction wave progressively appears at -0.950 V (Figure S6B in the Supporting Information). This behavior is indicative of the relatively low stability of Ni_5 in this buffer. Unlike Ni_5 , the larger Ni_{14} is stable in various media. Figure 6 features the CVs

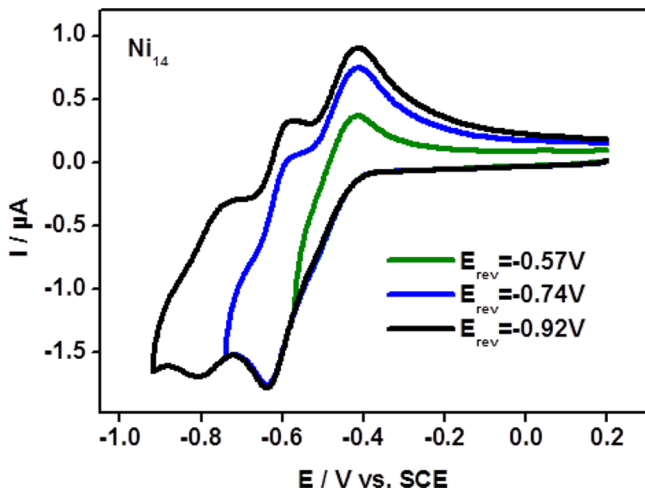


Figure 6. Cyclic voltammograms obtained at different reverse potentials with a 5×10^{-5} M solution of Ni_{14} in 1 M $\text{LiCH}_3\text{COO}/\text{CH}_3\text{COOH}$, $\text{pH} = 4$, at 10 mV s^{-1} .

of Ni_{14} obtained at 10 mV s^{-1} , at different reverse potentials, in a pH 4 acetate medium. The CVs are restricted to the two chemically reversible W-reduction waves peaking at -0.638 and -0.808 V vs SCE, respectively. The first wave is composite, as revealed by the presence of a reduction shoulder at ca. -0.510 V vs SCE, but its deconvolution was not observed even at a scan rate as small as 2 mV s^{-1} . In contrast, two well-separated oxidation waves are observed on potential reversal at -0.418 and -0.578 V vs SCE, respectively, thus confirming the composite nature of the first cathodic W-wave. These chemically reversible processes are diffusion-controlled as revealed by the peak current dependence on the square root of the scan rate (Figure 7). The second W-wave is followed by a large intensity wave (not shown) which is a combination of irreversible multielectron reduction of Ni_{14} and electrolyte discharge. Reductive deposition processes are associated with this wave. Such phenomena have been described for different POMs.^{9,34}

The exact positions and number of the W-reduction waves evolve upon increasing the pH of the supporting electrolyte (Figure 8). As expected, the whole CV pattern moves toward negative potentials when the pH increases. Table 2 contains the CV characteristics of these waves and the peak potential differences as a function of pH. Considering just the reduction scan, the W-waves gradually merge when the pH is sequentially increased from 4 to 6. Interestingly, the single reduction wave observed at pH 6 is not completely deconvoluted even at scan rates as slow as 2 mV s^{-1} (Figure 9). This observation is remarkable because usually W-waves are more likely to split rather than merge upon increasing the electrolyte pH. The same behavior as a function of pH has been previously reported, namely, for the large, macrocyclic $[\text{H}_7\text{P}_8\text{W}_{48}\text{O}_{184}]^{33-}$ and for a few other polyanions,³⁵ and was rationalized by an inversion of some pK_a values upon reduction.³⁶ Indeed, it is well-known in POM electrochemistry that a multiple electron uptake often proceeds through either an electrochemical-

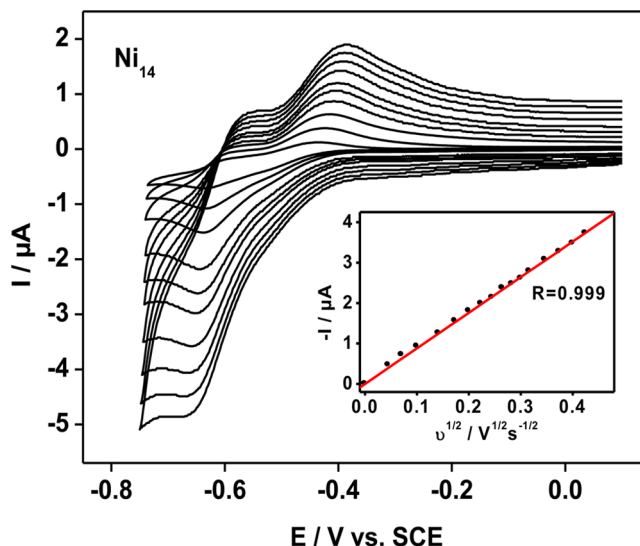


Figure 7. Cyclic voltammograms as a function of the scan rate for a 5×10^{-5} M solution of Ni_{14} in 1 M $\text{LiCH}_3\text{COO}/\text{CH}_3\text{COOH}$, $\text{pH} = 4$. Inset: cathodic peak current intensity variation as a function of the square root of the scan rate.

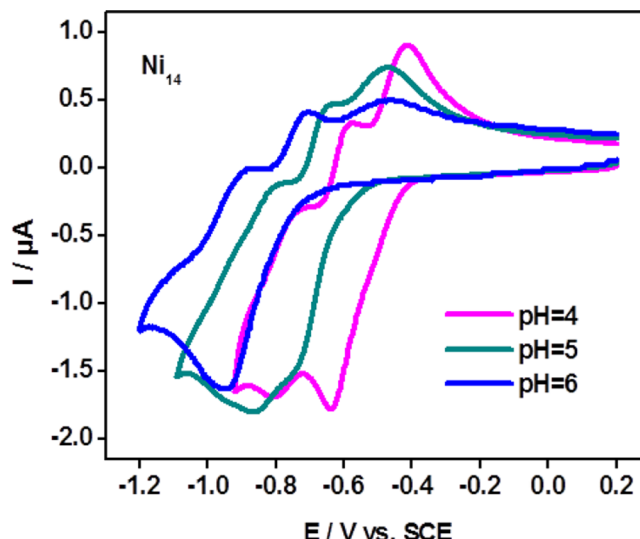


Figure 8. Comparison of the cyclic voltammograms obtained with 5×10^{-5} M solutions of Ni_{14} in 1 M $\text{LiCH}_3\text{COO}/\text{CH}_3\text{COOH}$, $\text{pH} = 4, 5$, and 6, at 10 mV s^{-1} .

chemical-electrochemical (ECE)- or an electrochemical-electrochemical-chemical (EEC)-type process, in which the chemical steps are protonations.³³ It is worth noting that proton consumption is already observed when Ni_{14} is dissolved in media with a mediocre buffer power in agreement with previous results obtained with other, large polyanions.³⁵⁻³⁷ A test carried out with Ni_{14} in a 1 M lithium chloride solution revealed that the pH increased from 3.31 up to 3.92 when a solution having a concentration as low as 1.3×10^{-5} M was prepared, corresponding to a striking 30 proton uptake per polyanion. This hints at the fact that Ni_{14} may work as an efficient proton reservoir and could turn out to be particularly suitable for the hydrogen-evolution reaction (HER), as described in the literature for other POMs.³⁸ In fact, controlled potential coulometry, performed at -0.670 V vs SCE, revealed that the number of electrons transferred to each Ni_{14} depends

Table 2. Anodic (E_{pa}) and Cathodic (E_{pc}) Peak Potentials and Their pH Shifts (ΔE_{pa} and ΔE_{pc}) for the Electron Transfer Processes Discussed in the Text^a

pH	E_{pa}	E_{pc}	ΔE_{pa}^b	ΔE_{pc}^b
4	-0.418	~−0.510		
	-0.578	-0.638		
	-0.724	-0.808		
5	-0.466		-0.048	
	-0.636	-0.740	-0.058	-0.102
	-0.792	-0.870	-0.068	-0.062
6	-0.460		-0.042	
	-0.702		-0.124	
	-0.864	-0.948	-0.140	-0.310

^aThe values are taken from voltammograms recorded at 10 mV s^{−1}. All values are in V vs SCE. ^bThe different potential shifts were calculated with respect to the results obtained at pH = 4.

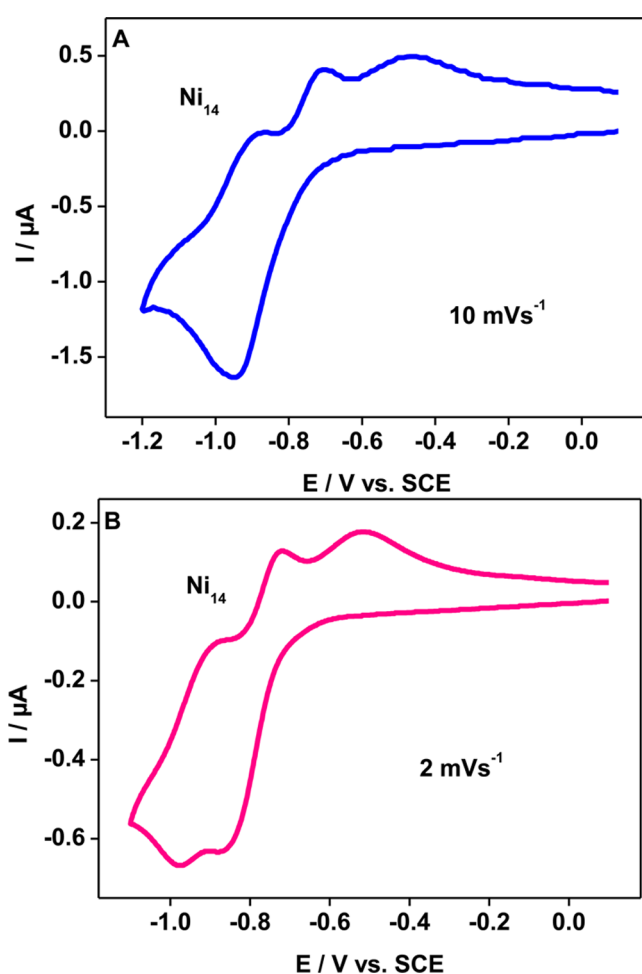


Figure 9. Comparison of the cyclic voltammograms obtained with a 5×10^{-5} M solution of Ni_{14} in 1 M $\text{LiCH}_3\text{COO}/\text{CH}_3\text{COOH}$, pH = 6, at scan rates of (A) 10 mV s^{−1} and (B) 2 mV s^{−1}.

on the number of available protons in the medium. For example, at pH 4 and at a concentration of 1.3×10^{-4} M for Ni_{14} , up to 16 electrons were consumed. The electrocatalytic proton reduction by reduced forms of Ni_{14} prevents the determination of the exact number of electrons related to the W-waves by controlled potential coulometry.

CONCLUSIONS

We have successfully synthesized two novel nickel(II)-containing heteropolytungstate derivatives by interaction of Ni^{2+} ions with the trilacunary $[\text{P}_2\text{W}_{15}\text{O}_{56}]^{12-}$ and the dilacunary $[\gamma\text{-GeW}_{10}\text{O}_{36}]^{8-}$ in slightly basic aqueous medium. These polyanions were characterized by single-crystal X-ray diffraction, IR spectroscopy, thermogravimetric analysis, elemental analysis, electrochemistry, and magnetic measurements. The 14- Ni^{2+} -containing 60-tungsto-12-phosphate(V) $[\text{Ni}_{14}(\text{OH})_6(\text{H}_2\text{O})_{10}(\text{HPO}_4)_4(\text{P}_2\text{W}_{15}\text{O}_{56})_4]^{34-}$ (Ni_{14}) was prepared using a simple, one-pot procedure by reacting $[\text{P}_2\text{W}_{15}\text{O}_{56}]^{12-}$ with Ni^{2+} ions in a pH 8 phosphate buffer. The novel polyanion Ni_{14} is composed of four Wells-Dawson type $\{\text{Ni}_3\text{P}_2\text{W}_{15}\}$ subunits encapsulating a central $\{\text{Ni}_2(\text{OH})_4(\text{H}_2\text{O})(\text{PO}_4)_4\}$ group resulting in a tetrameric aggregate. To date, Ni_{14} represents the largest nickel–oxo–hydroxo cluster in POM chemistry. The 5- Ni^{2+} -containing 17-tungsto-2-germanate(IV) $[\text{Ni}_5(\text{OH})_4(\text{H}_2\text{O})_4(\beta\text{-GeW}_9\text{O}_{34})(\beta\text{-GeW}_8\text{O}_{30}(\text{OH}))]^{13-}$ (Ni_5) was also prepared using a simple, one-pot procedure by reacting $[\gamma\text{-GeW}_{10}\text{O}_{36}]^{8-}$ with Ni^{2+} ions in an aqueous pH 8 medium. The sandwich-type Ni_5 comprises two nonequivalent lacunary Keggin units linked by a hydroxo-bridged, pentanickel(II) magnetic core. Dominant ferromagnetic interactions are present in both Ni_{14} and Ni_5 . Electrochemical studies show that Ni_{14} and Ni_5 give rise to chemically reversible responses in cyclic voltammetry (CV) which are attributed to the W centers. The two main reduction waves of Ni_{14} progressively merged upon increasing the pH, which is attributed to an acidity inversion effect between redox centers upon reduction.

ASSOCIATED CONTENT

Supporting Information

Infrared spectra, thermograms, UV-vis spectra, and cyclic voltammograms for NaRb-Ni_{14} and K-Ni_5 . Ball-and-stick representations of Ni_{14} and Ni_5 as well as crystallographic data in CIF format. Tables listing the BVS values of the protonated oxygens in Ni_{14} and Ni_5 . This material is available free of charge via the Internet at <http://pubs.acs.org>.

AUTHOR INFORMATION

Corresponding Author

*U.K.: e-mail, u.kortz@jacobs-university.de; fax, +49 421 200 3229; tel, +49 421 200 3235. A.K.P.: e-mail, annie.powell@kit.edu; fax, +49 721 608 48142; tel, +49 721 608 42135.

Notes

The authors declare no competing financial interest.

ACKNOWLEDGMENTS

U.K. thanks the German Science Foundation (DFG-KO-2288/3-2) and Jacobs University for research support. M.I. thanks DAAD and the Higher Education Commission of Pakistan for a doctoral fellowship, and the University of Balochistan, Quetta, Pakistan, for allowing her to pursue Ph.D. studies at Jacobs University (Germany). P.d.O. and B.K. thank the Université Paris Sud and the Centre National de la Recherche Scientifique (CNRS) for research support. Y.L. and A.K.P. acknowledge support from the CFN. Figures 1–4 were generated by Diamond, Version 3.2 (copyright Crystal Impact GbR).

■ REFERENCES

- (1) (a) Sartorel, A.; Bonchio, M.; Campagna, S.; Scandola, F. *Chem. Soc. Rev.* **2013**, *42*, 2262. (b) Izarova, N. V.; Pope, M. T.; Kortz, U. *Angew. Chem., Int. Ed.* **2012**, *51*, 9492. (c) Clemente-Juan, J. M.; Coronado, E.; Gaita-Ariño, A. *Chem. Soc. Rev.* **2012**, *41*, 7464. (d) Lv, H.; Geletti, Y. V.; Zhao, C.; Vickers, J. W.; Zhu, G.; Luo, Z.; Song, J.; Lian, T.; Musaev, D. G.; Hill, C. L. *Chem. Soc. Rev.* **2012**, *41*, 7572. (e) Long, D. L.; Tsunashima, R.; Cronin, L. *Angew. Chem., Int. Ed.* **2010**, *49*, 1736. (f) *Eur. J. Inorg. Chem.* **2009**, No. 34 (Issue dedicated to Polyoxometalates; Kortz, U., Guest Ed.), 5055–5276. (g) Kortz, U.; Müller, A.; van Slageren, J.; Schnack, J.; Dalal, N. S.; Dressel, M. *Coord. Chem. Rev.* **2009**, *253*, 2315. (h) Hasenkopf, B.; Micoine, K.; Lacôte, E.; Thorimbert, S.; Malacria, M.; Thouvenot, R. *Eur. J. Inorg. Chem.* **2008**, *5001*. (i) Cronin, L. In *Comprehensive Coordination Chemistry II*, Vol. 7; McCleverty, J. A.; Meyer, T. J., Eds.; Elsevier: Amsterdam, 2004; p 1. (j) *Chem. Rev.* **1998**, *98*, No. 1 (Special Issue on Polyoxometalates; Hill, C. L., Ed.), 1–390. (k) Hill, C. L.; Prosser-McCartha, C. M. *Coord. Chem. Rev.* **1995**, *143*, 407.
- (2) (a) Pope, M. T.; Kortz, U. Polyoxometalates. In *Encyclopedia of Inorganic and Bioinorganic Chemistry*; Scott, R. A., Ed.; John Wiley: Chichester. DOI: 10.1002/9781119951438.eibc0185.pub2. (b) Zhang, F.-Q.; Guan, W.; Yan, L.-K.; Zhang, Y.-T.; Xu, M.-T.; Hayfron-Benjamin, E.; Su, Z.-M. *Inorg. Chem.* **2011**, *50*, 4967. (c) Müller, A.; Roy, S. *Coord. Chem. Rev.* **2003**, *245*, 153. (d) *Polyoxometalates: From Platonic Solids to Antiretroviral Activity*; Pope, M. T.; Müller, A. *Angew. Chem., Int. Ed. Engl.* **1991**, *30*, 34. (f) Pope, M. T. *Heteropoly and Isopoly Oxometalates*, Springer-Verlag: Berlin, 1983.
- (3) Examples include the following: (a) Bassil, B. S.; Ibrahim, M.; Al-Oweini, R.; Asano, M.; Wang, Z.; van Tol, J.; Dalal, N. S.; Choi, K.-Y.; Biboum, R. N.; Keita, B.; Nadjo, L.; Kortz, U. *Angew. Chem., Int. Ed.* **2011**, *50*, 5961. (b) Zheng, S. T.; Zhang, J.; Clemente-Juan, J. M.; Yuan, D.-Q.; Yang, G.-Y. *Angew. Chem., Int. Ed.* **2009**, *48*, 7176. (c) Mal, S. S.; Bassil, B. S.; Ibrahim, M.; Nellutla, S.; van Tol, J.; Dalal, N. S.; Fernández, J. A.; López, X.; Poblet, M. J.; Ngo Biboum, R.; Keita, B.; Kortz, U. *Inorg. Chem.* **2009**, *48*, 11636. (d) Kortz, U.; Müller, A.; van Slageren, J.; Schnack, J.; Dalal, N. S.; Dressel, M. *Coord. Chem. Rev.* **2009**, *253*, 2315. (e) Mal, S. S.; Dickman, M. H.; Kortz, U.; Todea, A. M.; Merca, A.; Bögge, H.; Glaser, T.; Müller, A.; Nellutla, S.; Kaur, N.; van Tol, J.; Dalal, N. S.; Keita, B.; Nadjo, L. *Chem.—Eur. J.* **2008**, *14*, 1186. (f) Fang, X.; Kögerler, P. *Chem. Commun.* **2008**, 3396. (g) Godin, B.; Chen, Y.; Vaissermann, J.; Ruhlmann, L.; Verdaguier, M.; Gouzerh, P. *Angew. Chem., Int. Ed.* **2005**, *44*, 3072. (h) Bassil, B. S.; Nellutla, S.; Kortz, U.; Stowe, A. C.; van Tol, J.; Dalal, N. S.; Keita, B.; Nadjo, L. *Inorg. Chem.* **2005**, *44*, 2659. (i) Coronado, E.; Giménez-Saiz, C.; Gómez-García, C. J. *Coord. Chem. Rev.* **2005**, *249*, 1776. (j) Mialane, P.; Dolbecq, A.; Marrot, J.; Rivière, E.; Sécheresse, F. *Angew. Chem., Int. Ed.* **2003**, *42*, 3523. (k) Coronado, E.; Giménez-Saiz, C.; Gómez-García, C. J.; Laukhin, V. *Nature* **2000**, *408*, 447.
- (4) (a) Klöwer, F.; Lan, Y.; Nehrkorn, J.; Waldmann, O.; Anson, C. E.; Powell, A. K. *Chem.—Eur. J.* **2009**, *15*, 7413. (b) Stamatatos, T. C.; Abboud, K. A.; Wernsdorfer, W.; Christou, G. *Angew. Chem., Int. Ed.* **2008**, *47*, 6694. (c) Xu, J. Y.; Qiao, X.; Song, H. B.; Yan, S. P.; Liao, D. Z.; Gao, S.; Journaux, Y.; Cano, J. *Chem. Commun.* **2008**, 6414. (d) Fang, X. K.; Kögerler, P. *Chem. Commun.* **2008**, 3396. (e) Murugesu, M.; Clérac, R.; Wernsdorfer, W.; Anson, C. E.; Powell, A. K. *Angew. Chem., Int. Ed.* **2005**, *44*, 6678. (f) Murugesu, M.; Clérac, R.; Anson, C. E.; Powell, A. K. *Inorg. Chem.* **2004**, *43*, 7269. (g) Murugesu, M.; Anson, C. E.; Powell, A. K. *Chem. Commun.* **2002**, 1054.
- (5) (a) Zheng, S.-T.; Yang, G.-Y. *Chem. Soc. Rev.* **2012**, *41*, 7623. (b) Oms, O.; Dolbecq, A.; Mialane, P. *Chem. Soc. Rev.* **2012**, *41*, 7497.
- (6) (a) Huang, L.; Zhang, J.; Cheng, L.; Yang, G.-Y. *Chem. Commun.* **2012**, *48*, 9658. (b) Li, X.-X.; Zheng, S.-T.; Fang, W.-H.; Yang, G.-Y.; Clemente-Juan, J. M. *Chem.—Eur. J.* **2011**, *17*, 13032. (c) Zheng, S.-T.; Zhang, J.; Yang, G.-Y. *Angew. Chem., Int. Ed.* **2009**, *48*, 7176.
- (7) Zhang, H.; Li, Y.; Lu, Y.; Clérac, R.; Zhang, Z.; Wu, Q.; Feng, X.; Wang, E. B. *Inorg. Chem.* **2009**, *48*, 10889.
- (8) Clemente-Juan, J. M.; Coronado, E.; Galán-Mascarós, J. R.; Gómez-García, C. J. *Inorg. Chem.* **1999**, *38*, 55.
- (9) Pichon, C.; Mialane, P.; Dolbecq, A.; Marrot, J.; Rivière, E.; Bassil, B. S.; Kortz, U.; Keita, B.; Nadjo, L.; Sécheresse, F. *Inorg. Chem.* **2008**, *47*, 11120.
- (10) Zhang, Z. M.; Li, Y. G.; Wang, E. B.; Wang, X. L.; Qin, C.; An, H. Y. *Inorg. Chem.* **2006**, *45*, 4313.
- (11) Zhang, Z. M.; Wang, E. B.; Qi, Y. F.; Li, Y. G.; Mao, B. D.; Su, Z. *M. Cryst. Growth Des.* **2007**, *7*, 1305.
- (12) (a) Yang, L.; Huo, Y.; Niu, J. *Dalton Trans.* **2013**, *42*, 364. (b) Zhao, J. W.; Zhang, J.; Song, Y.; Zheng, S. T.; Yang, G. Y. *Eur. J. Inorg. Chem.* **2008**, 3809. (c) Zheng, S.-T.; Yuan, D.-Q.; Zhang, J.; Jia, H.-P.; Yang, G.-Y. *Chem. Commun.* **2007**, 1858. (d) Zhao, J.-W.; Jia, H.-P.; Zhang, J.; Zheng, S.-T.; Yang, G.-Y. *Chem.—Eur. J.* **2007**, *13*, 10030.
- (13) (a) Nsouli, N. H.; Prinz, M.; Damnik, N.; Neumann, M.; Talik, E.; Kortz, U. *Eur. J. Inorg. Chem.* **2009**, 5096. (b) Liu, X.-M.; Wang, C.-R.; Liu, B.; Xue, G.-L.; Hu, H.-M.; Wang, J.-W.; Fu, F. *Chin. J. Chem.* **2005**, *23*, 1413. (c) Mbomekalle, I. M.; Keita, B.; Nierlich, M.; Kortz, U.; Berthet, P.; Nadjo, L. *Inorg. Chem.* **2003**, *42*, 5143. (d) Kortz, U.; Mbomekalle, I. M.; Keita, B.; Nadjo, L.; Berthet, P. *Inorg. Chem.* **2002**, *41*, 6412. (e) Kortz, U.; Tézé, A.; Hervé, G. *Inorg. Chem.* **1999**, *38*, 2038. (f) Gómez-García, C. J.; Coronado, E.; Ouahab, L. *Angew. Chem., Int. Ed.* **1992**, *31*, 649.
- (14) Boyd, T.; Mitchell, S. G.; Miras, H. N.; Long, D.-L.; Cronin, L. *Dalton Trans.* **2010**, *39*, 6460.
- (15) (a) Yao, S.; Zhang, Z.; Li, Y.; Wang, E. *Dalton Trans.* **2010**, *39*, 3884. (b) Zhang, Z.; Yao, S.; Li, Y.; Wang, Y.; Qi, Y.; Wang, E. *Chem. Commun.* **2008**, 1650.
- (16) (a) Schaming, D.; Canny, J.; Boubekeur, K.; Thouvenot, R.; Ruhlmann, L. *Eur. J. Inorg. Chem.* **2009**, 5004. (b) Gómez-García, C. J.; Borrás-Almenar, J. J.; Coronado, E.; Ouahab, L. *Inorg. Chem.* **1994**, *33*, 4016.
- (17) Contant, R.; Tézé, A. *Inorg. Chem.* **1985**, *24*, 4610.
- (18) Mal, S. S.; Kortz, U. *Angew. Chem., Int. Ed.* **2005**, *44*, 3777.
- (19) Bassil, B. S.; Ibrahim, M.; Mal, S. S.; Suchopar, A.; Ngo Biboum, R.; Keita, B.; Nadjo, L.; Nellutla, S.; van Tol, J.; Dalal, N. S.; Kortz, U. *Inorg. Chem.* **2010**, *49*, 4949.
- (20) Finke, R. G.; Droege, M. W.; Domaille, P. J. *Inorg. Chem.* **1987**, *26*, 3886.
- (21) Nsouli, N. H.; Bassil, B. S.; Dickman, M. H.; Kortz, U.; Keita, B.; Nadjo, L. *Inorg. Chem.* **2006**, *45*, 3858.
- (22) SAINT; Bruker AXS Inc.: Madison, WI, 2007.
- (23) (a) Sheldrick, G. M. *Acta Crystallogr.* **2007**, *A64*, 112. (b) Sheldrick, G. M. SADABS; University of Göttingen: Göttingen, Germany, 1996.
- (24) Sheldrick, G. M. SHELX-97, *Program for Solution of Crystal Structures*; University of Göttingen: Göttingen, Germany, 1997.
- (25) Keita, B.; Nadjo, L. *J. Electroanal. Chem.* **1988**, *243*, 87.
- (26) (a) Pradeep, C. P.; Long, D.; Kögerler, P.; Cronin, L. *Chem. Commun.* **2007**, 4254. (b) Hussain, F.; Bassil, B. S.; Bi, L.-H.; Reicke, M.; Kortz, U. *Angew. Chem., Int. Ed.* **2004**, *43*, 3485.
- (27) (a) Lydon, C.; Sabi, M. M.; Symes, M. D.; Long, D.-L.; Murrie, M.; Yoshii, S.; Nojiri, H.; Cronin, L. *Chem. Commun.* **2012**, *48*, 9819. (b) Ibrahim, M.; Lan, Y.; Bassil, B. S.; Xiang, Y.; Suchopar, A.; Powell, A. K.; Kortz, U. *Angew. Chem., Int. Ed.* **2011**, *50*, 4708. (d) Pichon, C.; Dolbecq, A.; Mialane, P. R.; Marrot, J.; Rivière, E.; Sécheresse, F. *Dalton Trans.* **2008**, *71*. (c) Wu, Q.; Li, Y.; Wang, Y.; Wang, E.; Zhang, Z.; Clérac, R. *Inorg. Chem.* **2009**, *48*, 1606–1612.
- (28) (a) Ibrahim, M.; Mal, S. S.; Bassil, B. S.; Banerjee, A.; Kortz, U. *Inorg. Chem.* **2011**, *50*, 956. (b) Fang, X.; Kögerler, P. *Angew. Chem., Int. Ed.* **2008**, *47*, 8123. (c) Al-Kadamany, G.; Hussain, F.; Mal, S. S.; Dickman, M. H.; Leclerc-Laronze, N.; Marrot, J.; Cadot, E.; Kortz, U. *Inorg. Chem.* **2008**, *47*, 8574. (d) Zhao, J.; Zhang, J.; Zheng, S.; Yang, G. *Inorg. Chem.* **2007**, *46*, 10944. (e) Müller, A.; Döring, J. Z. *Anorg. Allg. Chem.* **1991**, *595*, 251.
- (29) Brown, I. D.; Altermatt, D. *Acta Crystallogr.* **1985**, *B41*, 244.
- (30) (a) Assran, A. S.; Mal, S. S.; Izarova, N. V.; Banerjee, A.; Suchopar, A.; Sadakane, M.; Kortz, U. *Dalton Trans.* **2011**, *40*, 2920.

- (b) Bassil, B. S.; Kortz, U. *Dalton Trans.* **2011**, *40*, 9649. (c) Bassil, B. S.; Dickman, M. H.; Kortz, U. *Inorg. Chem.* **2006**, *45*, 2394. (d) Mialane, P.; Dolbecq, A.; Marrot, J.; Rivière, E.; Sécheresse, F. *Chem.—Eur. J.* **2005**, *11*, 1771. (e) Kortz, U.; Isber, S.; Dickman, M. H.; Ravot, D. *Inorg. Chem.* **2000**, *39*, 2915. (f) Mayer, C. R.; Fournier, I.; Thouvenot, R. *Chem.—Eur. J.* **2000**, *6*, 105. (g) Wassermann, K.; Lunk, H. J.; Palm, R.; Fuchs, J.; Steinfeldt, N.; Stosser, R.; Pope, M. T. *Inorg. Chem.* **1996**, *35*, 3273. (h) Tézé, A.; Hervé, G. *Inorg. Synth.* **1990**, *27*, 85. (i) Canni, J.; Tézé, A.; Thouvenot, R.; Hervé, G. *Inorg. Chem.* **1986**, *25*, 2114.
- (31) (a) Nsouli, N. H.; Ismail, A. H.; Helgadottir, I. S.; Dickman, M. H.; Clemente-Juan, J. M.; Kortz, U. *Inorg. Chem.* **2009**, *48*, 5884. (b) Bassil, B. S.; Kortz, U.; Tigan, A. S.; Clemente-Juan, J. M.; Keita, B.; de Oliveira, P.; Nadjo, L. *Inorg. Chem.* **2005**, *44*, 9360.
- (32) Ngo Biboum, R.; Nanseu Njiki, C. P.; Zhang, G.; Kortz, U.; Mialane, P.; Dolbecq, A.; Mbomekalle, I. M.; Nadjo, L.; Keita, B. *J. Mater. Chem.* **2011**, *21*, 645.
- (33) Keita, B.; Nadjo, L. *Electrochemistry of Polyoxometalates, Encyclopedia of Electrochemistry*; Bard, A. J., Stratmann, M., Eds.; Wiley-VCH: 2006; Vol. 7, p 607.
- (34) Keita, B.; Nadjo, L. *Mater. Chem. Phys.* **1989**, *22*, 77.
- (35) Keita, B.; Lu, Y. W.; Nadjo, L.; Contant, R. *Electrochim. Commun.* **2000**, *2*, 720.
- (36) Lisnard, L.; Mialane, P.; Dolbecq, A.; Marrot, J.; Clemente-Juan, J. M.; Coronado, E.; Keita, B.; de Oliveira, P.; Nadjo, L.; Sécheresse, F. *Chem.—Eur. J.* **2007**, *13*, 3525 and references therein.
- (37) Keita, B.; de Oliveira, P.; Nadjo, L.; Kortz, U. *Chem.—Eur. J.* **2007**, *13*, 5480.
- (38) (a) Nohra, B.; El Moll, H.; Rodriguez Albelo, L. M.; Mialane, P.; Marrot, J.; Mellot-Draznieks, C.; O’Keefe, M.; Ngo Biboum, R.; Lemaire, J.; Keita, B.; Nadjo, L.; Dolbecq, A. *J. Am. Chem. Soc.* **2011**, *133*, 13363. (b) Keita, B.; Kortz, U.; Brudna Holzle, L. R.; Brown, S.; Nadjo, L. *Langmuir* **2007**, *23*, 9531.